Journal of Materials Science Research and Reviews

5(4): 18-36, 2020; Article no.JMSRR.59397

Application of Activated Eggshell as Effective Adsorbent in the Removal of Lead (II) Ion from Fertilizer Plant Effluent

Onoh Ikechukwu Maxwell[1], Mbah Gordian Onyebuchukwu[1], Ejikeme Euphemia Ifechukwu[1], Thompson Chime Onyejiuwa[1], Asadu Christain Oluchukwu[2*] and Ejikeme-Ezechi Margret[3]

[1]Department of Chemical Engineering, Enugu State University of Science and Technology (ESUT), P.M.B. 01660, Enugu, Nigeria.
[2]Department of Chemical Engineering, Gregory University Uturu, P.M.B 1012, Abia State, Nigeria.
[3]Department of Chemical Sciences, Godfrey Okoye University, Ugwuomu-Nike, Enugu, Nigeria.

Authors' contributions

This work was carried out in collaboration among all authors. Authors OIM, MGO and EEI designed the study, performed the statistical analysis, wrote the protocol and wrote the first draft of the manuscript. Authors TCO and ACO managed the analyses of the study. Author EEI managed the literature searches. All authors read and approved the final manuscript.

Article Information

Editor(s):
(1) Dr. Oscar Jaime Restrepo Baena, Universidad Nacional de Colombia, Colombia.
Reviewers:
(1) Foujan Falaki, Islamic Azad University, Iran.
(2) Monier Morad Wahba, National Research Centre, Egypt.
Complete Peer review History: http://www.sdiarticle4.com/review-history/59397

Original Research Article

Received 17 May 2020
Accepted 23 July 2020
Published 01 August 2020

ABSTRACT

The adsorption of lead (II) ions from fertilizer wastewater using Acid Modified Eggshell (AMES) as adsorbents was studied. The effects of process parameters such as temperature, contact time, pH and adsorbent dosage on the adsorption of Lead (II) ions from fertilizer industrial waste water were investigated. FTIR spectrum was employed to investigate the functional groups present in the egg shell before and after modification. Scanning Electron Microscope (SEM) was used to study the surface morphology of the egg shell before and after modification. Kinetic and isotherm model of the best fit for the data was investigated using the established models. FTIR characterization revealed that some functional groups disappeared while new ones appeared after modification indicating effective modification. SEM analysis revealed that the microporous spaced increased

**Corresponding author: Email: a.christian@gregoryuniversityuturu.edu.ng;*

after modification. The process factors considered significantly affected the rate of lead ion adsorption. Batch adsorption studies demonstrated that the highest percentage of 94.6% of lead ion was removed at a dosage of 40 mg of adsorbent per 100 ml of effluent after 60mins at a pH of 5 with optimum temperature of 45°C. The adsorption isotherm suggested a good fit of the experimental data into Temkin models with 0.998 as the R^2 value. Second order kinetic model was found to be the best fit for the adsorption data. Thermodynamic studies revealed that the adsorption of lead ion onto activated egg shell is endothermic with entropy and enthalpy value as 0.025 kJ/mol.k and 15.96 kJ/mol, respectively. Results obtained showed that acid modified egg shell is a good adsorbent for the removal of lead ion from wastewater.

Keywords: Eggshell adsorbent; lead (II) ion; adsorption; thermodynamics; Isotherm.

1. INTRODUCTION

The natural beauty of the environment is been challenged with improper waste disposal. Waste management has been a major issue in the developed, developing and under developed countries of the world. Most of these wastes are generated from different sources such as residents, hospitals, industries, commercial, automobiles, agriculture, institutions, construction and demolition sites. Apparently, most agricultural waste can be reduced, reused and recycled into new material for industrial consumption. Egg shell an agricultural waste is a common waste material generated from households, hatcheries and fast-food eateries [1]. Its disposal constitutes a major environmental issue as it involves odor, cost, abrasiveness, flies and availability of disposal sites [1]. Although, egg shell can be processed into commercial products such as fertilizer used for agricultural purpose [2], as adsorbent in waste water treatment [3], in the production of hydroxyapatite [4], and as a catalyst in chemical reactions [4]. The extract from the collagen shell membranes has various uses in medicine, cosmetics, food, biochemical and pharmaceutical industries [5]. Thus, this aforementioned uses of egg shell has reduced their environmental pollution menace [5].

Effluent emitted from Fertilizer industries is also an agent of environmental pollution. Effluent from various fertilizer plants includes various contaminates such as alcohols, salts and acids. It is characterized by high Chemical Oxygen Demand (COD) and ammonical nitrogen, reliant on the source of generation [1,6].

Adsorption is a technological process use in the removal of organic contaminant in effluent treatment. It is a mechanism by which a solid adsorbent can adsorb an adsorbate from an aqueous phase to its surface by forming an attachment through a physical or chemical bond, thereby removing the component from the aqueous phase [7,8]. Activated carbon is the conventional adsorbent usually used due to its relative ease of regeneration, large adsorption capacity and fast adsorption kinetics [8].

The uses of activated carbon as an adsorbent are enormous as the rise in demands has limited supply, which leads to the scarcity and expensiveness of the material [9-11]. This development calls for the exploration of cheap and affordable source of activated carbon with preferred characteristics such as; micro- or meso porosity or both, high surface area, depending on the end application, chemical composition, carbon purity, adsorptive capacity, thermal stability and surface functionality [12,13]. This research is particularly important considering that adsorption techniques is very simple to carry out when compared with other methods of separation and the adsorbent (egg shell) is available at no cost. Thus, this investigation seeks to explore the effectiveness of treating fertilizer plant effluent with activated carbon prepared from egg shell bio-waste.

2. MATERIALS AND METHODS

2.1 Reagents

All chemical reagents used were of analytical grade. These chemicals were used as such without further purification.

2.2 Sample Collection

The effluent was collected from Ebonyi State fertilizer plant in Izzi Local Government Area, Ebonyi State, Nigeria. The effluent was collected at earlier hours of the day in amber coloured specimen bottles. The effluent was immediately taken to the laboratory for physicochemical analysis and stored at ambient temperature.

Since the analysis of the sample was not immediately possible, the effluent was preserved in a refrigerator at 4°C. At this temperature, bacterial are in-active and biodegradation is inhibited [2].

2.3 Effluent Analysis

The effluent was analyzed before the adsorption experiment with egg shell adsorbent as described in the standard methods for effluent analysis [2,14]. The pH of the effluent was determined using a standard electronic pH meter (model: PHS – 3C) [8]. The turbidity of the effluent was determined using electronic turbidity meter manufactured by Labscience England (model: SGZ-200BS) [8]. Electrical conductivity of the effluent was measured by using table top conductivity meter manufactured by MetlerToledo (model: DDS – 307A CONDUCTIVITY METER), [5,8].

Dissolved Oxygen (DO) and Biochemical Oxygen Demand (BOD) was measured using table top dissolved oxygen meter manufactured by Hanna Instruments, Romania. Total Solids (TS), Total Suspended Solids (TSS) and Total Dissolved Solids (TDS) values were obtained using gravimetric method according to [8,9].

Acidity sulphate and chloride content of the waste water was determined using titrimetric method as described by [7]. Nitrate was determined using Spectrophotometry (SPECTIONIC-20) at 410 nm wavelength while Phosphate analysis was carried out using the UV spectrophotometer (spectrumlab 23 A) at 650 nm wavelength [15,14].

2.4 Adsorbent Preparation

The eggshells were obtained from Dennis Bakery industry in Abakaliki, Ebonyi state, Nigeria. The eggshells were washed and dried in a hot-air oven at about 40°C for 30 minutes to avoid denaturing of the protein content in the eggshell [10]. The dried eggshells were milled properly to fine powder to ensure a large surface area. The ground egg shells were sieved using 250 µm aperture sieve.

About 100 g of the ground bio-solid (< 250 µm mesh size) was carbonized in a muffle furnace at a temperature of 500°C for four hours after which they were allowed to cool. This process continued until a considerable quantity of carbonized samples was obtained [16,17]. The carbonized samples were washed in 10% V/V HCl solution in order to remove the surface ash. Then, it was washed by hot-water, before rinsing it with distilled water, to ensure complete removal of residual acid [15]. The solids were sun dried, before it was oven dried at 100°C for 1 hour [18,19].

For activation of the sample, approximately 50 g of the carbonized sample of 250 µm mesh-size was mixed with 100 ml of 1M activating agent (phosphoric acid). The sample mixtures were placed in a reflux system and heated at 900°C for two hours. Then, it was filtered and dried at 105°C in an oven. The samples were dried and subjected into an incinerator at 500°C for four hours. The activated sample generated was allowed to cool and washed or rinsed with 10% V/V HCl solution [15] in order to removed surface-ash, before preceded by warm water. Rinsing was done with distilled water to remove residual acid [15,20]. The samples were then dried in an oven at 110°C overnight and ball milled into dimensions/sizes that could pass via both less than 250 µm sieves. Washing process completed when a pH range of about 6-8 was attained [3,6].

$$\text{Activated Carbon yield} = W_1 / W_o \times 100$$

Where W_1 is the sample weight after carbonization and activation, and W_o is the sample initial weight.

2.5 Adsorbent Characterization

The raw, carbonized and acid modified egg shell was characterized for fixed carbon, ash content, surface area, bulk density, iodine number, moisture content and volatile content according to the methods outlined by [5,7,16]. The morphology and the surface chemistry of the egg shell were studied using Scanning Electron Microscope (SEM) instrument, manufactured by SEI with mode number 2250 and Fourier transform infrared spectrometer (FTIR) instrument, manufactured by AGILENT TECHNOLOGIES with model number CARY 630.

2.6 Adsorption Experiments

2.6.1 The effect of dosage

The Dosage effect of take-up ability/adsorption and the degree of taking out of lead (II) ion using acid modified egg shell activated carbon was

studied by stirring 10 g of the activated carbon with 100 ml of 27.9 mg/l of the lead (II) solution at about 40°C, for 60 minutes. The concentration of lead remaining in solution was measured at 556nm using UV spectrometer. The process was repeated with 20, 30, 40 and 50 g of the activated carbons.

2.6.2 The effect of pH

The pH of the fertilizer effluent of lead ion was varied with drops of 1M HCl and 1M NaOH solutions. The pH was measured using the pH meter. It was also noted that the pH of 3, 4, 5, 6, 8, 9 and 11 were prepared and used for the experiments by mixing 40mg of the adsorbent with 100 ml of 27.9 mg/l of the adsorbate in a water bath with shaker at 40°C and 60 minutes.

2.6.3 The effect of time

Observable effect of period/contact time on the take-up of lead (II) ion using the acid modified egg shell (AMES) was investigated by mixing 40mg of the adsorbent with 100 ml of 27.9 mg/l of the adsorbate in a water bath with shaker at room temperature at a neutral pH and for 10, 20, 30, 40, 50 and 60 minutes respectively.

2.6.4 The effect of temperature

The effects of the varied temperature were investigated by mixing 40 mg of the acid modified egg shell with 100 ml of 27.9 mg/l of the adsorbate in a water bath set at 30˚C and stirred for 60 minutes. Then, the solution was filtered and the absorbance was measured at 556 nm. The concentration was evaluated from the standard graph. The process was repeated with temperature set at 30, 35, 40, 45 and 50°C respectively.

2.7 Adsorption Kinetics

The kinetics process for the adsorption of lead (II) ion in the fertilizer wastewater was investigated using different kinetics models such as; Pseudo-first-order, Pseudo-Second-order, Elovich equation and Weber Morris kinetics model.

2.7.1 Pseudo first order kinetics

The linear form of the Lagergren or pseudo first order kinetics equation is given in Equation 1 [21,17,20,6]

$$\log(q_e - q_t) = logq_e - \left(\frac{k_1 t}{2.303}\right) \quad (1)$$

Where

q_e = equilibrium adsorption capacity (mg/g)
q_t = instantaneous adsorption capacity (mg/g)
k_1 = pseudo-first-order adsorption constant (min^{-1})

2.7.2 Pseudo second order kinetics

This model is based on the theory that chemisorptions is the rate determining step [22].

$$\frac{t}{q_t} = \frac{1}{k_2 q_e^2} + \frac{t}{q_e} \quad (2)$$

Where k_2= pseudo second order adsorption constant (g/mg min).

The calculated adsorption capacity qe_{cal} is obtained from the slope of the plot of t/q_t against t while k_2 is obtained from the intercept.

2.7.3 Elovich model

This model was originally developed for adsorption of gases on solid surfaces but it also provides a good model for solid-liquid or solid–solid adsorption [23].

$$q_t = \frac{1}{\beta} ln(\alpha\beta) + \frac{1}{\beta}\ln(t) \quad (3)$$

Where α = initial sorption rate constant (mg/g min) and β (g/mg) is related to the extent of surface coverage and the activated energy for chemisorptions.

2.7.4 Weber morris kinetics model

This model provides indices of the intraparticle diffusion rate (k_d) and boundary layer effect (l).The larger the l, the greater the contribution of surface sorption in the rate determining step.

$$q_t = k_d t^{1/2} + l \quad (4)$$

Where

k_d = intra-particle diffusion rate constant (mg/g $min^{½}$)
l = the boundary layer effect (mg/g)

2.8 Adsorption Isotherms

The adsorption isotherms used to model the adsorption of heavy metals are Langmuir, Freundlich, Temkin and Dubinin-Radushkevich Isotherm models.

2.8.1 Langmuir isotherm

This isotherm was based on the theory that took place in monolayer surface coverage. The linear form of the Langmuir isotherm is given in Equation 5.

$$\frac{C_e}{q_e} = \frac{1}{q_l k_l} + \frac{C_e}{q_l} \quad (5)$$

Where

$q_l =$ Monolayer adsorption capacity (mg/g)
$k_l =$ Langmuir adsorption constant (L/mg)

Langmuir isotherm provides a dimensionless quantity known as separation factor R_l that reflects the nature of the adsorption process. The equation for calculating R_l is given in Equation 6.

$$R_l = \frac{1}{[1+K_l C_o]} \quad (6)$$

Where C_o is the initial concentration of the adsorbate (ppm)

2.8.2 Freundlich isotherm

The linear form of this isotherm is given in Equation 7.

$$\log q_e = log k_f + {}^{1}/_{n}\, log C_e \quad (7)$$

Where

K_f = Freundlich adsorption constant (mg/g) $(mg/l)^{1/n}$
n = adsorption index, reflecting the intensity of the adsorption. If n lies between 1 and 10, it indicates a favorable adsorption [24].

2.8.3 Temkin isotherm

This Isotherm takes into description the interaction between adsorbents and metal ions based on the theory that the free energy of sorption is a function of the surface coverage. The linear form of this isotherm is as shown in Equation 8 [17,25].

$$q_e = BlnA + BlnC_e \quad (8)$$

Where

$$B = {}^{RT}/_{b_{T,}} \quad (9)$$

B is related to the heat of adsorption.

A is the equilibrium binding constant (mg/L), $b_T \left(\frac{J.g}{Lmol}\right)$ is adsorption constant, R is the universal gas constant (8.314 J/mol. K), T is the absolute temperature of the adsorption process

2.8.4 Dubinin-radushkevich (R-D) isotherm

The linear form of this isotherm is given in Equation 10.

$$lnq_e = lnq_m - \beta\varepsilon^2 \quad (10)$$

Where

β is a coefficient related to the mean free energy of adsorption per mol of the metal ion (mol^2/J^2),
q_m is the theoretical saturation capacity (mg/g) and ε is the Polanyi potential expressed as:

$$\varepsilon = RTln\left(1 + {}^{1}/_{C_e}\right) \quad (11)$$

C_e is the equilibrium concentration (mg/l)

2.9 Thermodynamics of the Adsorption Process

The thermodynamic parameters that were applied to the system are the standard Gibb′s free energy change (ΔG°), the standard enthalpy change (ΔH°) and the standard entropy change (ΔS°). The standard Gibb′s free energy change would indicate if the process is spontaneous (ΔG°< 0), if the process is non-spontaneous (ΔG° > 0) or if the process is at equilibrium (ΔG° = 0). The standard enthalpy change would indicate if the process is endothermic (ΔH° > 0) or exothermic (ΔH° < 0). Moreover, the absolute value of the standard enthalpy change would indicate if the process is chemisorptions (80 < ΔH° < 200kJ/mol) or physiosorption (ΔH° < 80kJ/mol) [2,16,26]. The standard entropy change would indicate the degree of dis-orderliness of the process. The process is possible (ΔS° > 0) or not possible (ΔS°< 0). Equations 12 – 14 were used to calculate the thermodynamic parameters [26].

$$\Delta G° = RTlnK \quad (12)$$

$$K = \frac{C_a}{C_e} = \frac{C_o - C_e}{C_e} \quad (13)$$

$$\ln K = \frac{\Delta G^O}{RT} = \frac{-\Delta H^O}{RT} + \Delta S \quad (14)$$

Using Equation 14, a plot of lnK against the inverse of temperature produced a straight line where the standard enthalpy change was calculated from the slope and the standard entropy change was calculated from the intercept.

3. RESULTS AND DISCUSSION

3.1 Characterization of the Fertilizer Plant Waste Water

Table 1 below shows the result on the characterization of fertilizer plant waste water. It is observed from the table that the pH of the sample was highly alkaline due to the presence of inorganic compounds. The total suspended solid, turbidity, total solid, biochemical oxygen demand, total dissolved solid and chemical oxygen demand of the waste water sample were very high due to the presence of organic and inorganic compounds.

3.2 Percentage Yield of Activated Carbon

The activated carbons yield was calculated from sample weight after carbonization and activation (w_1) to its initial weight (w_o). Table 2 shows the percentage yield of carbons prepared at different carbonization temperatures and times. It was observed that the yield decreased with increase in temperature and time. [10-11,27] obtained 35.7% and 28.9% yield in carbonizing rice husk at 500°C and 600°C respectively. The low yield at high temperature was essentially due to the volatilization of the volatile constituents upon heating [27]. Maximum yield of 41.42% was recorded for Acid modified egg shell (AMES) at activation temperature of 500°C, and activation time of 1 hour.

Table 1. Results on the characterization of waste water sample

S/No	Parameters	Units	Fertilizer Effluent
1	PH	Nil	10.5
2	Colour	Nil	BROWN
3	Turbidity	FAU	41
4	Temperature	°C	30.3
5	Conductivity	µs/cm	321
6	TSS	mg/l	0.287
7	TDS (Pb^{2+})	mg/l	630
8	TS	mg/l	631.267
9	BOD	mg/l	42
10	COD	mg/l	143
11	DO	mg/l	1.2
12	Nitrate	mg/l	6.12
13	Phosphate	mg/l	0.076

Where: Total solid (TS), Total suspended solid (TSS), Biochemical oxygen demand (BOD), Chemical oxygen demand (COD)

Table 2. Result on the percentage yield of activated carbon

@ 500°C Time (minutes)	EGG SHELL		
	Initial weight (g)	Final weight (g)	% Yield
60	200	82.84	41.42
90	200	75.68	37.84
120	200	68.64	34.32
@600°C			
60	200	55.00	27.50
90	200	50.44	25.22
120	200	44.10	22.05
@700°C			
60	200	40.50	20.25
90	200	36.90	18.45
120	200	33.96	16.98

3.3 Characterization of the Egg Shell Adsorbents

From the Table 3 below, the experimental result reveals that the samples had low fixed carbon and high volatile contents; these suggested that the samples required activation. It was also observed that after carbonization and acid modification, the surface area and fixed carbon of the adsorbents increased showing that activation increases the adsorption capacity of adsorbents. This increase in surface area after carbonization agrees with the report by Okpe et al. [22]; Asadu et al. [23] and Nwabanne et al. [26].

3.3.1 Scanning electron microscopy (SEM) analysis

The surface morphologies of the eggshell carbon without chemical activation and with chemical activation were evaluated with the aid of SEM as shown in Figs. 1 and 2 below. The figures clearly revealed the microscopic surface structure of the materials. It was clear that the carbon particles are in the form of spheres with a wide range of sizes in the unmodified egg shell. But after chemical activation of the egg shell, it was observed that the surface of the carbon has been changed into new coarse structure, which shows that the acid created higher surface area by opening more pores in the carbon structure. These results were in conformation with the results obtained by [24,28], where it was observed that adsorption sites of carbonized groundnut shell improved significantly, when modified with acid.

3.3.2 Fourier transform infra-red spectroscopy (FTIR) analysis of the adsorbent

Fourier transform infrared (FTIR) spectra of the raw and modified biomass (egg shell) are presented in Tables 3 and 4. From Tables 3 and 4, it was observed that after acid modification of the egg shell, the major functional groups present were; (C-O-O-, O-H, N-H, C=C-C, C-H, C-Cl) which were very useful in structure determination; hydroxyl, phenols, carboxyl, anhydrides and pyrones groups were also important sorption sites. The above changes in the spectra may be ascribed to the interaction of the H_3PO_4 and NH_4Cl with the carboxyl, hydroxyl and amino acids present on the surface of the acid activated carbon. FTIR spectra of the treated raw materials loaded display a number of absorption peaks than the untreated raw materials.

Table 3. Result on the characterization of the egg shell (ES)

Adsorbents / Parameter	EGG SHELL (ES)		
	Raw	Carbonized	Acid modified Sample
Fixed Carbon (%)	10	63.73	71.28
Ash content (%)	6	1.93	1.36
Surface area (cm^2/g)	706.65	847.44	928.27
Bulk density (g/cm^2)	0.63	0.57	0.51
Iodine number (mg/g)	622.73	730.94	783.97
Moisture content (%)	0.48	0.26	0.31
Volatile content (%)	83.52	34.35	27.36

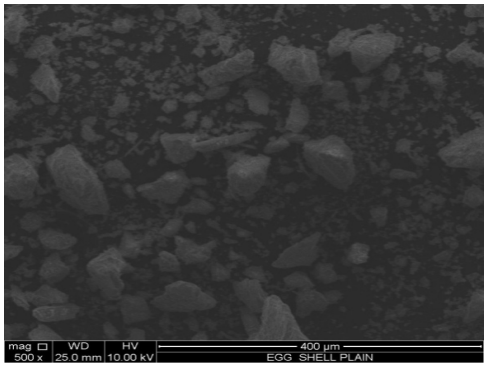

Fig. 1. Raw egg shell

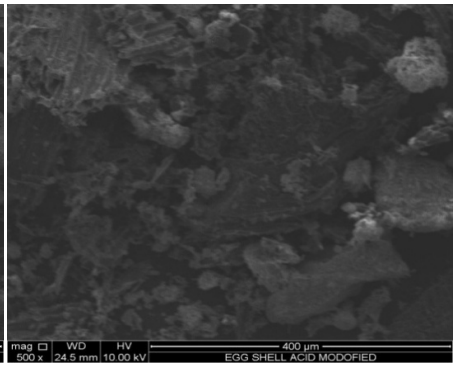

Fig. 2. Acid modified egg shell

Table 4. Fourier transform infrared spectrum for raw egg shell (RES)

RES wave number (cm^{-1})	Bond source
2109.7	C ≡ C Terminal alkyne (monosubstituted)
1796.6	C– H stretch in alkanes
1640.0	C- C stretch in alkynes
1405.2	C-H in plane bend in alkenes
1080	C – O stretch vibration of esters, ethers, anhydride, alcohol, carboxyl amide, C-C stretch.
903	C-H stretch, N-H rocking
872.2	PH bend in phosphines
711.9	N-H rocking, C-H rocking, C-Cl_2, C-Br.

Table 5. Fourier transform infrared spectrum for acid modified egg shell (AMES)

AMES wave number (cm^{-1})	Bond source
3805.59	O-H Stretch in phenols and alcohols
3690.1	O-H Stretch in phenols and alcohols
3533.5	O-H Stretch in phenols and alcohols
3473.9	Hydroxyl group, H-bonded OH stretch
3157.1	C=H stretch in alkenes
2922	C-H stretch of alkanes
2322	C=C stretch in alkynes
2105.9	Transition Metal carbonyl
1994.1	Aromatic Combination bands
1640.0	N-H bend in amines
1543.0	C=C stretch in aromatics
1200.2	O-H, Primary or secondary, OH in-plane bend
1118.2	C-O-C, Alkyl-substituted ether, C=O stretch
864.0	PH bend in phosphines

3.4 Effects of Process Parameters

3.4.1 Effect of adsorbent dosage

The effect of adsorbent dosage on the adsorbed percentage is presented in Fig. 3. The adsorbed percentage increased with increasing the adsorbent dosage to a maximum amount at a dosage of 40 mg/100 ml. Then, the adsorption percentage remained constant afterwards. It could be inferred that once the surface pores of the adsorbents are saturated with the adsorbate, the adsorption percentage can no longer increase, instead it may remain constant or possibly decline. This might be because of the excess over lapping of the active sites at increased concentration/dosage of the adsorbents, thus, decreasing the surface area [19,22]. However the percentage adsorbed by acid modified egg shell at 40 mg/100 ml dosage was 90.60%, which may be attributed to improved surface area and percentage fixed carbon of modified egg shell as shown in Table 2 of the Characterization of the egg shell (ES).

The above result is in accordance with the results observed from the adsorption of Pb^{2+} ion unto groundnut shell by Onwu et al. [28], where adsorbent dose range from 0.5 g to 1.75 g. The uptake of Pb^{2+} ion increased rapidly from 0.5 mg to 1.5 mg (per 50 ml of the solution) and marginally thereafter. Abudus et al. [1,24,25] observed sharp increase of Pb^{2+} ion adsorption with rise in the adsorbent dosage from 47.9% to 74.1%, then the effectiveness gradually increased to 91.55% with treat to 3.0g and utmost removal competence of 96.6% was obtained with 5.0 g of dosage.

3.4.2 Effect of pH

The hydrogen potential (pH) of the lead (II) solution to be adsorbed (adsorbate) was a significant factor in the adsorption processes. The pH of the aqueous solution affected the breaking up of the cation substituted groups on the adsorbent, constancy of metal complexes and formation of new species of metals during reaction [12,20]. The adsorption capability of the adsorbent increased with the pH, with maximum percentage adsorption observed at pH of 5. This region is a mild acidic region, and thus the highest adsorption capacity and percentage

adsorbed were recorded. The percentage adsorbed dropped towards the neutral region and increased slightly towards the mild alkaline region. Comparable results were obtained by [1], for the removal of arsenic by heat treated rice husk where percentage removal was maximum at pH 6 (mild acidic region). Also [11,22] observed the same behavior using untreated rice husk and groundnut shell in lead removal at different pH and noted that at pH 6, 1.0 g of rice husk (RH) was capable of removing 93.78% of lead, while at pH 5, 1.0 g of groundnut shell was efficient in the removal of 97.48% of lead.

It is also because of low pH, increase/high concentrations of H^+ ions are available in solution to contend for the vacant adsorption sites of adsorbents. This is shown by the sharp increase in the percentage removal at low pH values (pH 3 and 5). The higher adsorption effectiveness at near neutral (mild acidic region) can be attributed to lack of electrostatic repulsion between the

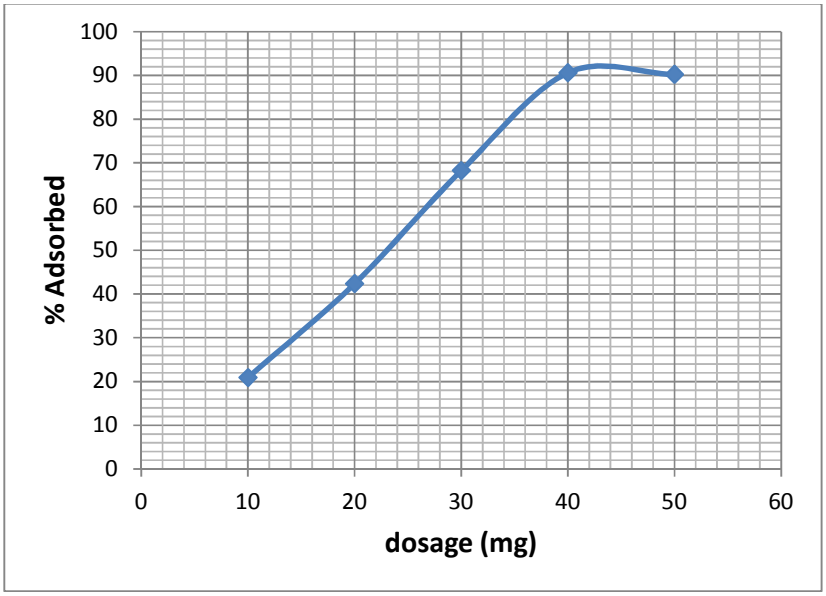

Fig. 3. Effect of adsorbent dosage on adsorption of Pb^{2+} on AMES

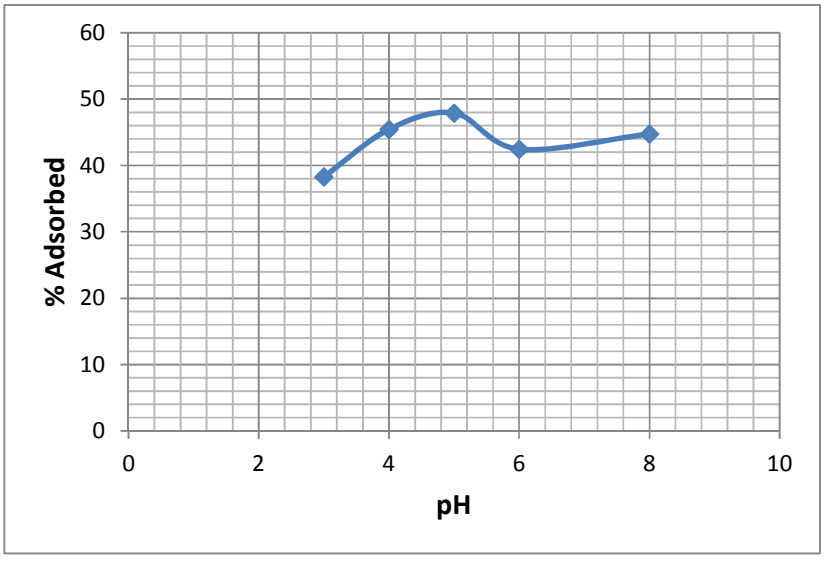

Fig. 4. Effect of pH on adsorption of P_b^{2+} on AMES

surface of adsorbents and Pb^{2+} species. Reduced trend in uptake was noted above pH of 5, maybe owing to formation of soluble hydroxyl complexes [21]. But this is contrary to the results obtained by [12,14] where the maximum removal efficiency was 57% at pH of 8. This could be as a result of lack of chemical treatment of the adsorbent.

3.4.3 Effect of time

The adsorption capacity increased with increasing of contact time and remained constant thereafter. Subsequent to 45 minutes of contact, it was discovered that the adsorption percentage remained constant. This effect of time may be due to the equilibrium of the adsorption process. Once equilibrium is attained, there will be no further increase in either adsorption capacity or removal percentage. The reduced adsorption rate was owed to the reduction in adsorption sites on the surface of the adsorbents [25]. The equilibrium adsorption capacity of the modified egg shell was observed 2.95 mg/g, which was the maximum adsorption capacity achieved in 45 minutes of contact time. The essence was that the adsorption process would not be carried on till infinity since the maximum percentage adsorption was achieved in 45 minutes, as presented in Fig. 5.

The results of Deepika et al. [12] showed that most of Pb^{+2} adsorptions had slower equilibrium time (2 to 3 hours) but in this study the rate of this phenomenon was faster and is comparable with the observation of Gupta et al. [29], where equilibrium time was recorded as 1hour. These variations in optimum contact time maybe associated with surface characteristics of the adsorbents.

3.4.4 Effect of temperature

The temperature of the adsorption was another factor that significantly affected the adsorption capacity of the adsorbent and removal percentage of lead (II) ion; however, the effect was the same on adsorption capacity and removal percentage because the process was carried out at the same dosage and concentration. Fig. 6 shows the effect of temperature on percentage adsorbed, where it can be seen that the percentage adsorbed increased with temperature to 45°C and remained constant afterward. At lower temperature the percentage adsorbed was low because the low kinetic energy of the molecules, while the kinetic energy of the molecules increased as the temperature increased, with observed optimum temperature of 45°C. At a relatively high temperature above 70°C the surface of the adsorbent and the active sites would be negatively affected by the temperature and the adsorption process would be slowed, resulting to low/declined percentage adsorption. Similar results were reported by Onwu et al. [27] and Onwu et al. [28].

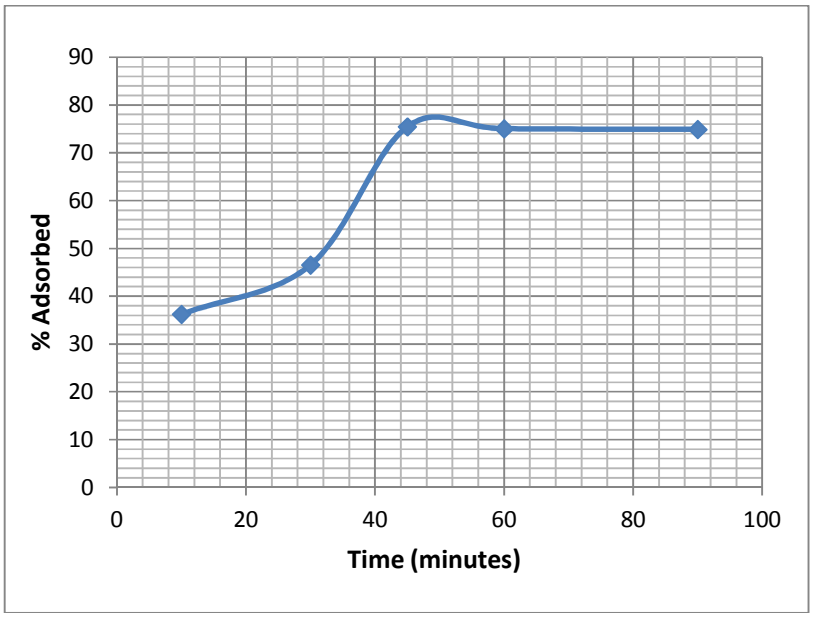

Fig. 5. Effect of Time on adsorption of P_b^{2+} ion on AMES

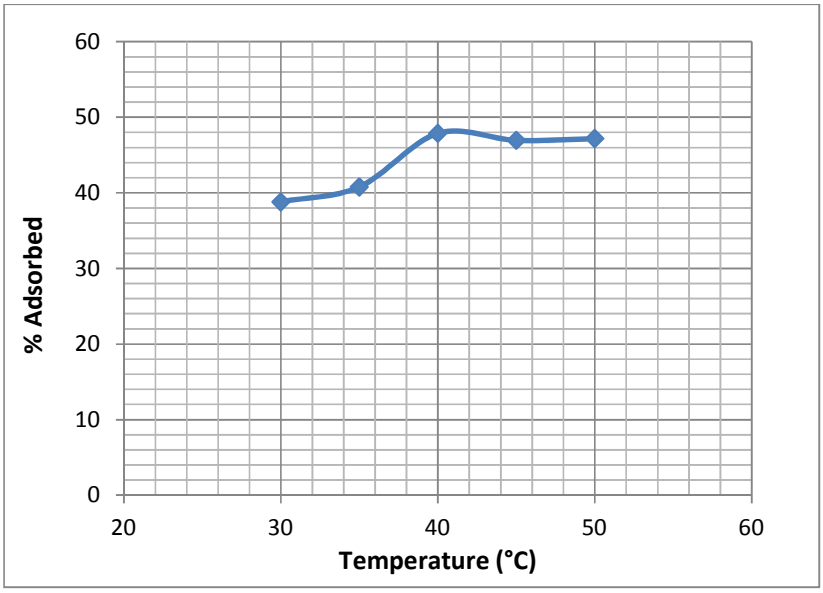

Fig. 6. Effect of temperature on adsorption of P_b^{2+} ion on AMES

3.5 Kinetics

3.5.1 First order kinetics or (pseudo first order)

The logarithm of the differences between the equilibrium adsorption capacity and instantaneous adsorption capacity was plotted against time according to Equation 1. The first-order kinetics constant was obtained from the slope of the plot while the calculated adsorption capacity was obtained by taking the antilogarithm of the intercept. The values of the first-order parameters were shown in Table 6. The value of the correlation coefficient (R^2) for the acid modified egg shell first-order (AMES) adsorption kinetic was 0.9101. This value was close enough to 1, therefore the experimental data fitted into the pseudo-first-order kinetics model. The observed equilibrium adsorption capacity of egg shell adsorbent was much higher than the calculated value. The difference was 1.86 mg/g.

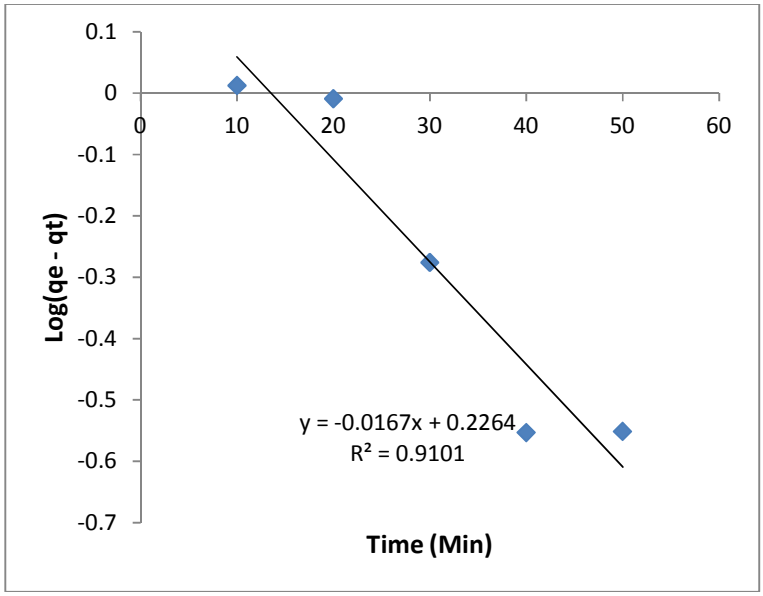

Fig. 7. First order kinetics for adsorption of $_{Pb}^{2+}$ on AMES

Table 6. The Kinetics parameter for the adsorption of lead ion onto AMES

	Acid modified Egg shell (ames) adsorbent			
1st Order	qe (Obs) (mg/g)	qe(cal) (mg/g)	K (min^{-1})	R^2
	3.78	1.92	0.044	0.9101
2nd Order	qe (Obs) (mg/g)	qe(cal) (mg/g)	K (g/mg min)	R^2
	3.50	4.27	0.029	0.983
Elovich	A (mg/gmin)	B (g/mg)		R^2
	3.57	1.55		0.861
Weber Morris	Kd ($mg/gmin^{1/2}$)	L (mg/g)		R^2
	0.278	1.741		0.928

3.5.2 Second order kinetics (pseudo-second-order)

The experimental data was modeled into the pseudo-second-order kinetics by plotting the ratio of time to instantaneous adsorption capacity against time according to Equation 2. The calculated adsorption capacity was obtained as the inverse of the slope while the second order kinetics constant was obtained from the intercept. The determined correlation coefficient value for the egg shell was 0.983. Hence, the experimental data fitted into the pseudo- second-order kinetic model was better than that of 1st order. The parameters were however provided in Table 6.

3.5.3 Elovich kinetics model

The instantaneous adsorption capacity was plotted against the logarithm of time to study the extent of the fitness of the experimental data into Elovich model according to Equation 3 .The constant β which is an indication of the extent of surface coverage was obtained as the inverse of the slope while the constant α which is the initial rate constant was obtained from the intercept. The determined correlation coefficient (R^2) was 0.861 for the egg shell adsorbent and can be accepted to a good extent. The Elovich Equation parameters were also given in Table 6.

3.5.4 Weber morris kinetics

The instantaneous adsorption capacity was plotted against the square root of time according to Equation 4. The determined correlation coefficient R^2 value was 0.928. The intraparticle diffusion rate constant K_d was obtained as the slope while the boundary layer effect (L) was obtained as the intercept. The K_d value for egg shell adsorbent was high which implies that the adsorption beyond surface was higher in egg shell. The parameters were also provided in Table 6.

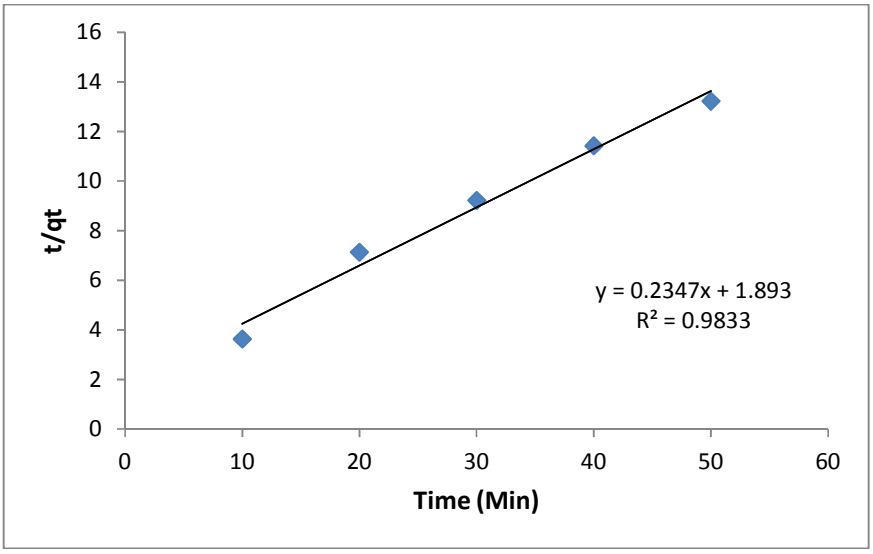

Fig. 8. The second order kinetics for adsorption of P_b^{2+} on AMES

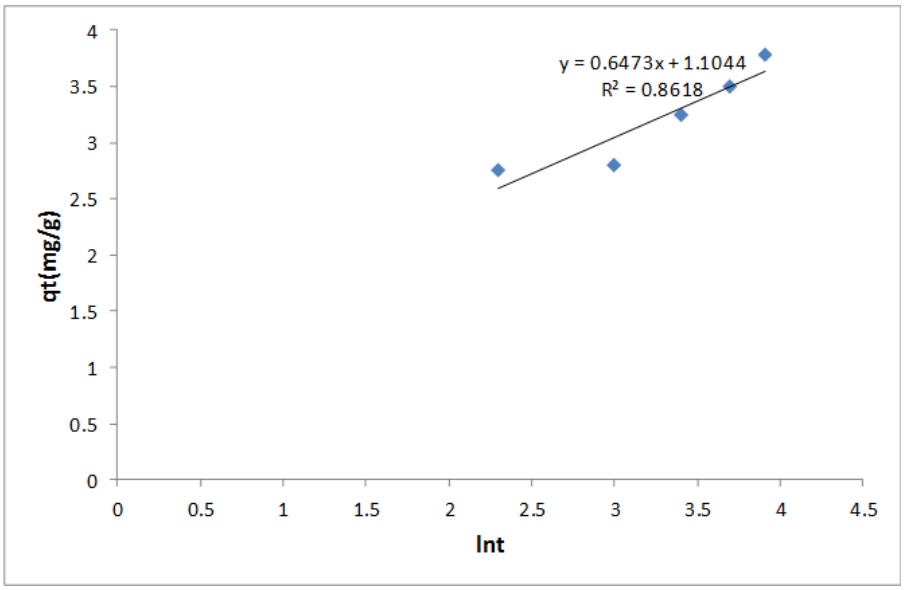

Fig. 9. Elovich Kinetics for adsorption of P_b^{2+} on AMES

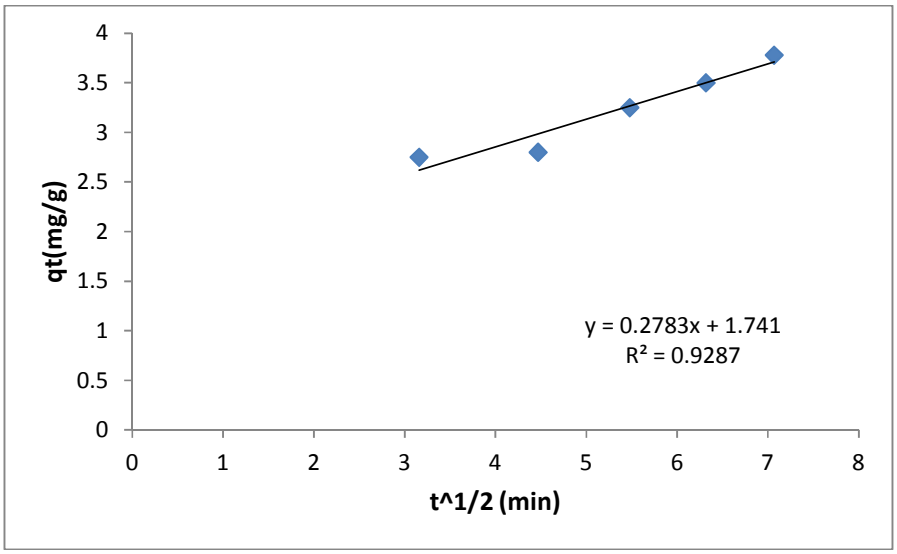

Fig. 10. Weber-morris kinetics for adsorption of Pb^{2+} on AMES

3.6 Adsorption Isotherms

3.6.1 Langmuir isotherm

The fitness of the experimental data into the Langmuir adsorption isotherm was investigated by plotting the ratios of the equilibrium concentration to the adsorption capacity against the equilibrium concentration according to Equation 5. The monolayer adsorption capacity was obtained as the inverse of the slope while the adsorption constant was obtained from the intercept. The determined coefficient R^2 was 0.9955 which suggested a good fit of the experimental data into the Langmuir adsorption isotherm. The monolayer adsorption capacity was 16.95 mg/g which correlates with the results obtained under the kinetic studies where it was discovered that the rate of adsorption with egg shell was high. The separation factor according to Equation 6 was observed to lie between 0 and 1 for the adsorption process. This confirms that the adsorption was favorable. The Langmuir parameters are presented in Table 7.

Table 7. The adsorption isotherm parameters for the adsorption of Pb^{2+} on AMES

		Egg shell	
Langmuir	ql(mg/g)	kl(L/mg)	R^2
	16.95	-0.109	0.995
Fruendlich	Kf(mg/g) $(mg/L)^{1/n}$	N	R^2
	1.18	2.18	0.932
Temkin	b_T(J.g/L.mol)	A(mg/L)	R^2
	-51.99	0.029	0.998
R-D	qm(mg/g)	β(mol^2/J^2)	R^2
	4.81	7E-07	0.888

3.6.2 Freundlich isotherm

The logarithm of the adsorption capacities at different initial concentration of Pb^{2+} was plotted against the logarithm of concentration according to Equation 7. The determined coefficient (R^2) value was 0.9327.The index n, which determines whether the adsorption was favorable or not, was determined from the inverse of the slope. The value of "n" was 2.18, this value lies between 1 and 10, denoting a favorable adsorption (Freundlich, 1906). The parameter for Freundlich isotherm is also presented in Table 7.

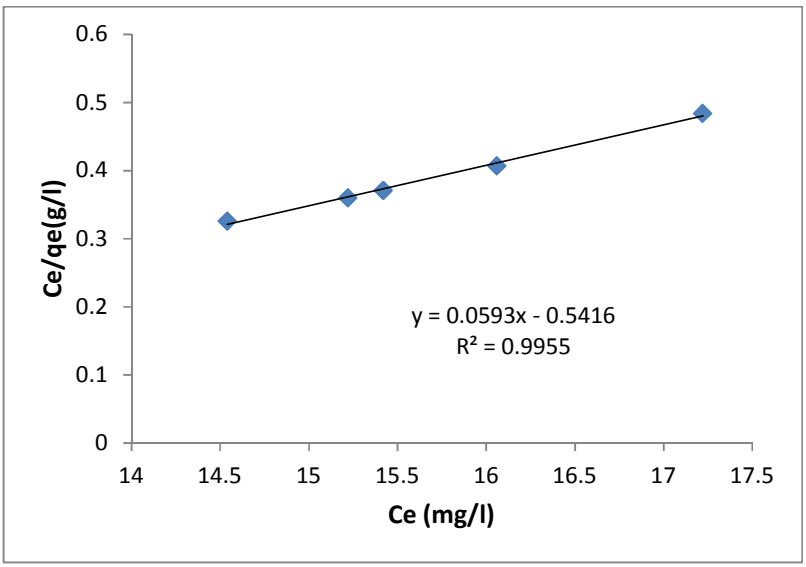

Fig. 11. Langmuir isotherm for adsorption of Pb^{2+} on AMES

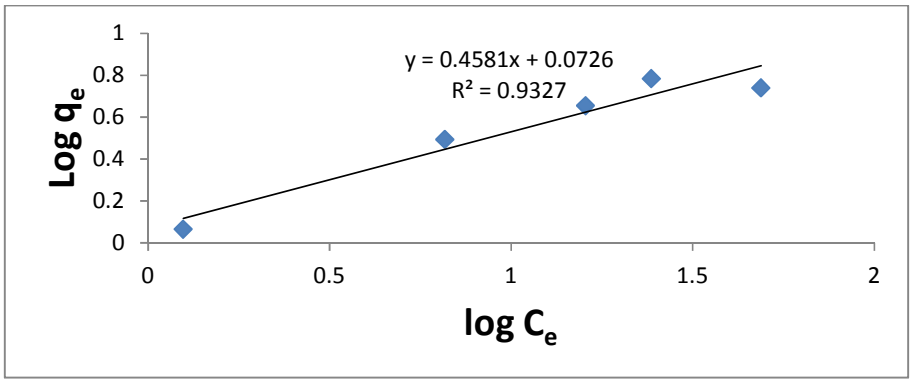

Fig. 12. Freundlich isotherm for adsorption of Pb^{2+} on AMES

3.6.3 Temkin isotherm

The adsorption capacities at different initial metal concentrations were plotted against the logarithm of the equilibrium concentration according to Equation 8. The experimental data provided a good fit with the Temkin isotherm as the determined coefficient R^2 value was close to 1. The Temkin Isotherm parameter is also presented in Table 7. The adsorption constant b_T was obtained from the slope and the temperature of the system according to Equation 10, while the equilibrium binding constant A was obtained from the intercept. The binding constant for egg shell was -52.16 (Jg/l). It can be seen from Table 7 above that Temkin model gives the best fit with R^2 of 0.997 for the egg shell.

3.6.4 Dubinin-radushkevich (R-D) isotherm

The experimental data was modeled into R-D isotherm by plotting the logarithm of the adsorption capacity at different initial metal concentrations against the square of the Polanyi potential according to Equation 10. The determined coefficient R^2 value was 0.8882. The coefficient related to the mean free energy of the adsorption per mole of the metal ion was obtained from the slope of the plot, while the theoretical saturation capacity was obtained from the intercept of the plot. The saturation capacity of the adsorption was high. The saturation capacity according to R-D model was close to the monolayer adsorption capacity according to the Langmuir isotherm.

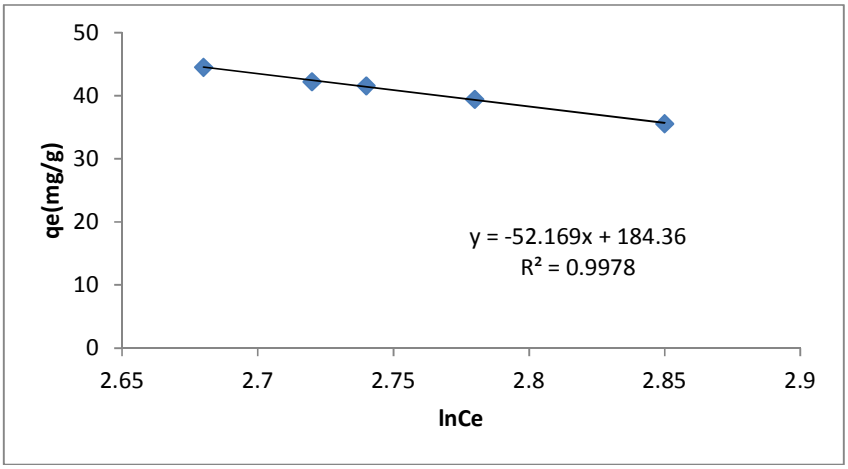

Fig. 13. Temkin isotherm for adsorption of Pb^{2+} on AMES

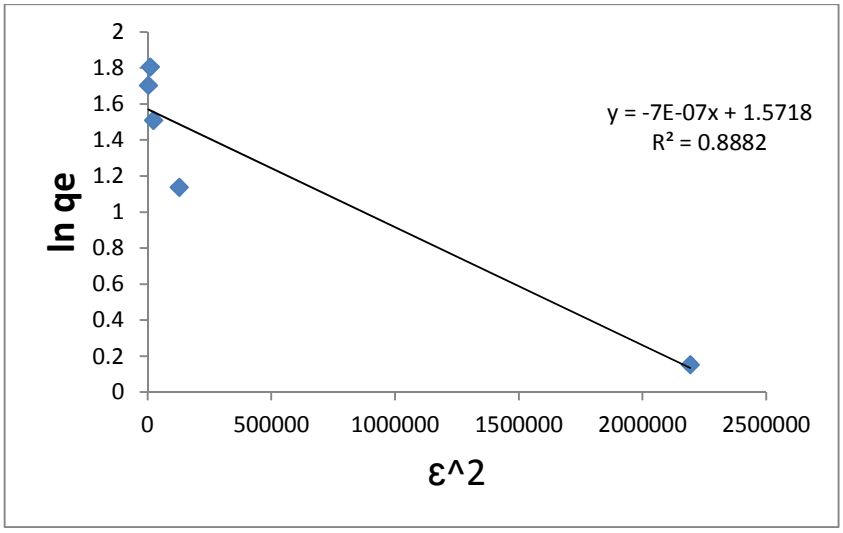

Fig. 14. Dubinin-radushkevich(R-D) isotherm for adsorption of Pb^{2+} on AMES

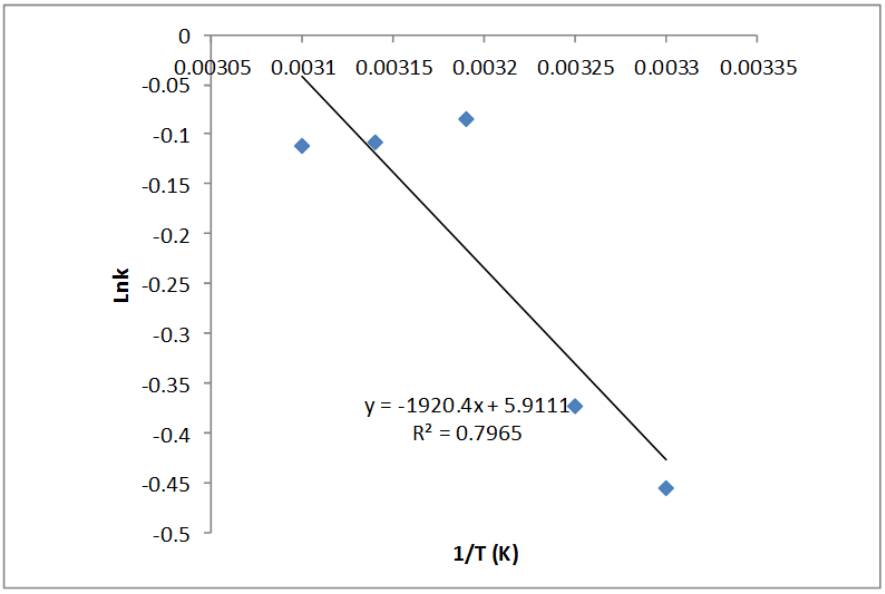

Fig. 15. The thermodynamics plot for the adsorption of Pb^{2+} on AMES

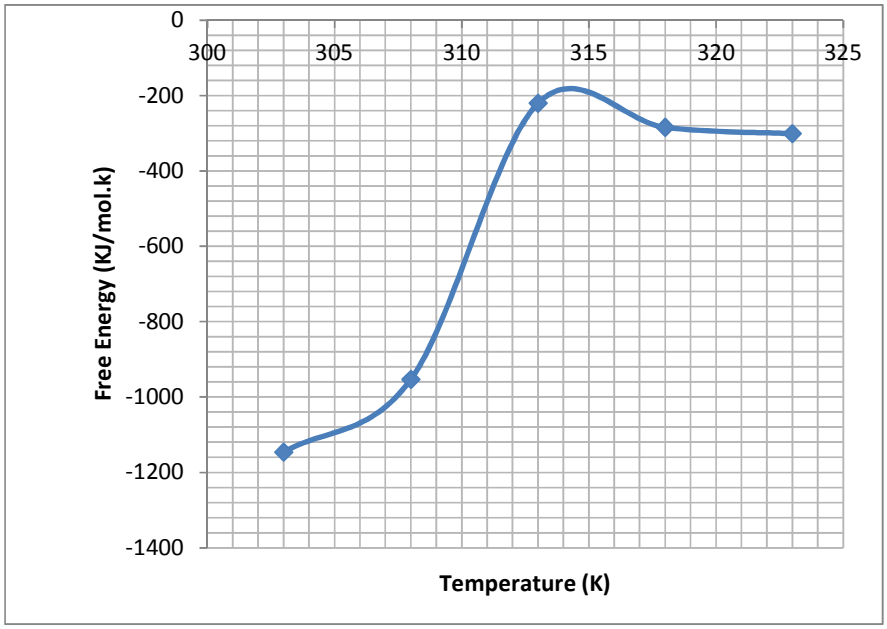

Fig. 16. Free energy versus temperature plots for the adsorption of Pb^{2+} on AMES

Table 8. Thermodynamic parameters for the adsorption of Pb^{2+} on AMES

		Egg shell		
Temp (K)	ΔG° (KJ/mol)	ΔH° (KJ/mol)	ΔS° (KJ/mol. K)	R^2
303	-1146.4	15.96	0.025	0.79
308	-953.30			
313	-220.30			
318	-284.44			
323	-300.90			

3.7 Thermodynamic Studies

The thermodynamics studies were carried out using Equations 12 - 14. The standard Gibb's free energy change (ΔG°) for the adsorption processes was obtained from Equation 12. The value of the standard Gibb's free energy change for the adsorption was negative showing that the adsorption process was spontaneous. The absolute values of the standard free energy change for the adsorption of Pb^{2+} with egg shell were negative and at the corresponding temperatures. This is another indication that the adsorption of Pb^{2+} with egg shell activated carbon was spontaneous. The standard enthalpy change (ΔH°) was obtained from the slope of the plot of the logarithm of the equilibrium constants against the inverse of absolute temperature according to Equation 14. The value of the standard enthalpy changes for the egg shell was positive meaning that the adsorption processes was endothermic. The standard enthalpy changes for egg shell was high, however the value was less than 80 kJ/mol showing that the adsorption was more of physical than chemical process. In other words, the adsorption can be reversed. The standard entropy change (ΔS°) was obtained from the intercept of the plot. The standard entropy changes for the egg shell was positive indicating an endothermic process. Fig. 16 shows the plot of free energy versus temperature for the Pb^{2+} adsorption with egg shell. It was observed from Fig. 16 that the absorption has the highest standard Gibb's free energy change (ΔG°) values of -220.30 KJ/mol and the adsorption processes occurred at an optimized temperature of 313k. The values of the standard Gibb's free energy change for the Pb^{2+} adsorption with egg shell were negative showing that the adsorption processes were spontaneous.

4. CONCLUSION

Egg shell an agricultural common waste material generated from households, hatcheries and fast-food eateries etc, was converted by carbonization and acid bakeries activation to a functional and efficient adsorbent material for the removal of Pb^{2+} from fertilizer waste water. The egg shell was carbonized at 500°C, 600°C and 700°C for 60 minutes, 90 minutes and 120 minutes respectively. Then, the carbonized egg shell was acid modified to enhance its adsorption capacity. The raw, carbonized and acid modified egg shell samples were characterized for fixed carbon, ash content, surface area, bulk density, iodine number, moisture content and volatile content. The effects of process parameters (temperature, contact time, pH and adsorbent dosage) on the adsorption of lead (II) ions from fertilizer industrial waste water were investigated and found significant. The adsorption rate parameters showed that the adsorption of Pb^{2+} ions using acid modified egg shell (AMES), as adsorbent, was a second -order- reaction. The adsorption isotherm suggested a good fit of the experimental data into the Langmuir and Temkin models.

COMPETING INTERESTS

Authors have declared that no competing interests exist.

REFERENCES

1. Abudus S, Takumi F, Ahmed HA, Dabawan H, Katsumata T, Suzuki M, Furukawa SK. Enhanced removal of arsenic from groundwater by adsorption onto heat- treated rice husk. Journal of Science and Technology. 2016;2(3):511-516.
2. Ademoroti CMA. Standard methods for waste and effluent analysis. Foludex Press Ltd. Ibadan, Nigeria. 1996;55-70.
3. Ahmedna M, Marshal W, Rao M. Production of granular activated carbon from selected Agric by products. Bioresource and Technology. 2000;71(2): 113–123.
4. Alagumuthu G, Rajan M. Kinetic and equilibrium studies on fluoride removal by zirconium (iv) impregnated groundnut shell carbon. Hemijska Industrija. 2010;64(1): 295-304.
5. Amadi BA, Agomuo EN, Ibegbulem CO. Research methods in biochemistry. Supreme Publishers, Owerri. 2004;90-115.
6. Vinay M. Bhandari, Laxmi Gayatri Sorokhaibam Vivek V. Ranade. Industrial wastewater treatment for fertilizer industry-A case study. Journal of desalination and Water Treatment. 2016;57(57):27934-27944.
   Available:http://www.tandfonline.com/doi/full/10.1080 /19443994. 2016.1 186399
7. Anirudhan TS, Radhakrishan PG. Thermodynamics and Kinetics of Adsorption of Cu(II) from Aqueous Solutions onto a new cation exchanger derived from tamarind fruit shell. Journal of Chemical Thermodynamics. 2008;40:702-709.

8. AOAC. Offical method of analysis of the association of official analytical chemists. 15th Ed. Washington USA; 2004.
9. APHA. Standard methods of water and waste water examination. 16th Edition, American Public Health Association (APHA), Washington DC, USA; 1992.
10. Arunlertaree C, Kaewsomboon W, Kumsopa A, Pokethitiyook P, Panyawathanakit P. Removal of lead from battery manufacturing wastewater by egg shell Songklanakarin. Journal of Science and Technology. 2007;29(3):857-868.
11. Asadullah K. Mohs Halim SI, Lias, Kamal Md. Shamsulzhar. Adsorption process of Heavy metals by low-cost Adsorbent: A review. World Applied Sciences Journal. 2013;28:1518-1530.
12. Deepika Haldhar, Sunanda sahoo, Mishra PC. Adsorption of As (III) from aqueous solution by groundnut shell. Indian Journal of Applied Research. 2014;1(4):270-273.
13. Viswanathan B, Indra Neel P, Varadarajan TK. "Methods of Activation and Specific Applications of Carbon Materials", National Centre for Catalyst Research, Indian Institute of Technology, Madras, Chennai. 2009;600(036).
Available:https://nccr.iitm.ac.in/e%20book-Carbon%20Materials%20final.pdf
14. Giri J. Fang, Deng B. Preparation and evaluation of GAC-based iron containing adsorbents for arsenic removal. Environmental Science Technology. 2012; 39(10):3833–3843.
15. Fan X, Parker DJ, Smith MD. Adsorption kinetics of fluoride on low cost materials. Water Research. 2003;37:4929–4937.
16. Itodo AU, Abdulrahman FW, Hassan LG, Maigandi SA, Happiness UO. Diffusion mechanism and kinetics of biosorption of textile dye by H3PO4 and ZnCl2 impregnated poultry wastes sorbents. International Journal of Natural and Applied Sciences. 2009;5(1):7-12.
17. Turoti M, Gimba C, Ocholi O, Nok A. Effect of different Activation Methods on the Adsorption Characteristics of Activated Carbon from *Khaya senegalensis* Fruits and Delonix Regia pods. Chemclass Journal. 2007;4:107–112.
18. Itodo AU, Abdulrahman FW, Hassan LG, Maigandi SA, Itodo HU. Application of Methylene Blue and Iodine Adsorption in the Measurement of Specific Surface Area by four Acid and Salt Treated Activated Carbons. New York Science Journal. 2010; 3(5):134–139.
19. Itodo AU, Abdulrahman FW, Hassan LG, Maigandi SA, Happiness UO. Thermodynamic equilibrium, kinetics and adsorption mechanism of industrial dye removal by chemically modified poultry droppings activated carbon. Nigerian Journal of Basic and Applied Science. 2009;17(1):38-43.
20. Udeozor SO, Evbuomwan BO. The Effectiveness of Snail Shell as Adsorbent For The Treatment of Waste Water From Beverage Industries Using H_3 PO_4 As Activating Agent. IOSR Journal of Engineering. 2014;4(8):37-41.
21. Kumar U, Bandyopadhyay M. Sorption of Cadmium from aqueous solution using pre-treated rice husk. Journal of Bioresources Technology 2006;97(1):104-109.
DOI: 10.1016/j.biortech.2005.02.027
22. Okpe Emmanuel Chinonye, Asadu Christian Oluchukwu, Onu Chijioke Elijah. Statistical analysis for orange G adsorption using kola nut shell activated carbon, Journal of the Chinese Advanced Materials Society; 2018.
Available:https://doi.org/10.1080/22243682.2018.1534607
23. Asadu CO, Onoh MI, Albert CA. Equilibrium isotherm studies on the adsorption of malachite green and lead ion from aqueous solution using locally activated ugwaka clay (black clay). Archives of Current Research International. 2018;12(2):1-11.
DOI: 10.9734/ACRI/2018/39302.
ISSN: 2454-7077.
24. Nwabanne JT, Okpe EC, Asadu CO, Onu CE. Sorption studies of dyestuffs on low-cost adsorbent. Asian Journal of Physical and Chemical Sciences. 2018;5(3):1-19.
25. Albert CA, Asadu CO, Onoh MI, Azubuike KA. Kinetics and isotherm studies on divalent lead ions adsorption by zeolite solution. Int'l Journal of Novel Research in Engineering and Science. 2016;3:49-61.
26. Nwabanne JT, Okpe EC, Asadu CO. Onu CE. Application of Response Surface Methodology in Phenol Red Adsorption Using Kola Nut (*Cola acuminata*) Shell Activated Carbon. International Research Journal of Pure & Applied Chemistry. 2017;15(4):1-14.
27. Onwu DO, Nick O, Cordelia ON, Asadu OO, CI, Maxwell O. Optimization of process parameters for the treatment of

crude oil spill polluting water surface by sorption technique using fatty acid grafted ogbono shell as a sorbent. Journal of Materials Science Research and Reviews. 2019;3(3):1-12.

28. Onwu DO, Ogbodo ON, Ogbodo NC, Chime TO, Udeh BC, Egbuna SO, Onoh MI, Asadu CO. Application of esterified ogbono shell activated biomass as an effective adsorbent in the removal of crude oil layer from polluting water surface. J. Appl. Sci. Environ. Manage. 2019;23(9): 1739-1746.
29. Gupta VK, Saini VK, Jain N. Adsorption of arsenic(111) from aqueous solutions by iron oxide-coated sand. Journal of Colloidal and Interace Science. 2005;288.

Peer-review history:
The peer review history for this paper can be accessed here:
http://www.sdiarticle4.com/review-history/59397